International Forum on Aeroelasticity and Structural Dynamics
IFASD 2017
25-28 June 2017 Como, Italy

POLYNOMIAL NONLINEAR STATE-SPACE MODELLING OF VORTEX-INDUCED VIBRATIONS: BLACK-BOX VS GREY-BOX APPROACH

J. Decuyper[1,3], J. P. Noël[2], T. De Troyer[3], M. C. Runacres[3], J. Schoukens[1]

[1]Department of Fundamental Electricity and Instrumentation (ELEC)
Vrije Universiteit Brussel
Pleinlaan, 2 Brussels 1050 Belgium
jan.decuyper@vub.be
johan.schoukens@vub.be

[2]Aerospace and Mechanical Engineering Department
University of Liège
Quartier Polytech 1 (B52/3), Allée de la deć ouverte, 9 Liège 4000 Belgium
jp.noel@ulg.ac.be

[3]Departement of Engineering Technology (INDI)
Vrije Universiteit Brussel
Pleinlaan, 2 Brussels 1050 Belgium
tim.de.troyer@vub.be
mark.runacres@vub.be

Keywords: Vortex-induced vibrations, Computational fluid dynamics, Polynomial nonlinear state-space modelling

Abstract: Polynomial nonlinear state-space (PNLSS) models have proven to be very useful in modelling highly nonlinear systems, encountered over a variety of engineering applications. In this work, we focus on modelling the kinematics of an oscillating circular cylinder, submerged in a low Reynolds number flow. Such a set up is typically used to study vortex shedding phenomena and their related forces. The power of the PNLSS model class comes from its large flexibility in candidate nonlinear basis functions. Flexibility, however, comes at a price. The number of parameters generally grows large, hampering the identification process and leading to a loss of insight in the nonlinear functions. The objective of this work is to investigate how prior knowledge of the nonlinearity can be introduced in the basis functions of these nonlinear models and how this affects the accuracy of the estimated model. In particular, the usage of polynomial functions in terms of states and the input is compared to nonlinear functions in terms of the output variable. An improved model was obtained when a deliberate choice of basis functions was chosen based on prior knowledge of the nonlinearity. In addition, promising results were obtained from using dedicated nonlinear basis functions in terms of the output on a system closely related to the vortex shedding system.

1 INTRODUCTION

The mutual interaction between flowing fluids and structures has been an important research topic for over decades. One particular form is called vortex-induced vibrations (VIV). Such

vibrations are especially known to occur for bluff bodies that are submerged in a fluid flow. In practice this can be a pipeline on the seabed, riser pipes from oil rigs but also chimneys exposed to wind, water channels in heat exchangers, bridges or aerofoils at large angle of attack. From an academic point of view often the shape of a circular cylinder is considered. Vibration is induced by shear layer instabilities which will lead to an alternating vortex shedding pattern in the wake of these structures for sufficiently high Reynolds number ($\mathrm{Re} > 49$) [1, 2]. With alternating vortex shedding, fluctuating pressure is associated. Consequently a fluctuating force is exerted on the structure. If the structure is flexible it will vibrate, hence vortex-induced vibrations.

Cases have been reported in which high amplitude vibrations have lead to severe damage, accelerated fatigue and even total collapse of structures [3]. Such events are usually encountered in the so-called lock-in range. This is a range where the frequency of oscillation and vortex shedding synchronise to a common frequency, typically in the neighbourhood of the eigenfrequency of the structure [4]. Lock-in can lead to a build up of energy with as a result high, possibly harmful amplitudes. Extensive reviews of the amplitude response encountered for, what are called freely oscillating cylinders, can be found in [5–7].

Given the consequences, there is a need for good predictions. Despite the substantial attention the topic of VIV has received over the past decades, analytical relations between the observed oscillations and the generated forces have only been deduced for a limited, and most often simplified (linearised) number of cases. The true relation remains hidden in the Navier-Stokes equations which require numerical integration to be solved, or dedicated labs for the solution to be observed. Both approaches are however unfit for a large number of applications, e.g. during the design process of a structure, for real-time health monitoring and foremost for control.

To overcome the downsides of time integration (computational fluid dynamics simulations), which is very computational expensive, people have resorted to low-order modelling. An interesting review of the classes of models which are frequently used for VIV is provided in [8]. Identifying a model relating the oscillation of, say a circular cylinder, to the observed forces onto the cylinder, is however not an easy task. The relationship is highly nonlinear: a bifurcation structure of non homogeneous solutions [9, 10] accompanied by hysteresis have been observed. Notice also that there exist already a stable oscillation of the lift force, even for the stationary cylinder case. This is also referred to as an autonomous oscillation. In recent years, techniques originally developed for modelling of electrical circuits and modal analysis have found their way to the fluid mechanics community [11, 12]. In [13] a nonlinear model relating the transverse oscillation of a cylinder, oscillating perpendicular onto the oncoming flow was related to the generated lift force. The flexible model class of polynomial nonlinear state-space [14] models was used to identify a model. Although accurate simulation results were obtained, also the pitfall of using such a flexible model structure had become apparent. Introducing a large number of degrees of freedom in the nonlinear basis functions (see Section 2.2) creates difficulties in obtaining good estimates of the parameters. This is due to the non convexness of the cost function. On the other hand, interesting results were obtained for the modelling of nonlinear structural vibrations by constructing dedicated nonlinear basis functions for state-space models [15]. The latter lead to a considerable reduction in the amount of parameters needed and to regaining insight in the nonlinearity itself.

In this work we seek to compare both the black-box identification approach, as was applied in [13] and the grey-box approach of [15]. As an intermediate step we will use the FAST-test [16] to characterise the type of nonlinearity and select the basis functions of the nonlinear

state-space model accordingly. Whenever any prior knowledge is introduced (as from the FAST-test) we will categorise the approach as being 'grey'. The lay-out of the paper is as follows: first the identification process, both for the fully black-box as for the grey-box approach is discussed. Next some attention is devoted to how the data were collected using CFD simulations. In what follows the results obtained from training models, with and without including prior knowledge in the basis functions, are presented for there estimation and validation and validating to new (unseen) data. Also the approach of creating dedicated basis functions is illustrated on data of the Van der Pol equation, an equation with related behaviour to the vortex shedding system. Finally some conclusions are provided.

2 THE IDENTIFICATION PROCESS

System identification typically is a four-step process. It is data-driven hence data needs to be collected. We also need to pick a model structure which we deem fit to be able to capture the observed behaviour. It then comes to matching the model as wel as possible to the data, given a certain quality criteria defined by the cost function. Finally, the obtained model is tested for its ability to reproduce data which was not used to fine tune the model (validation step).

Depending on the model structure, the parameter estimation problem differs. Therefore the two considered types, distinguished only by the choice of nonlinear basis functions, will be treated separately. The data which is used is identical.

2.1 Collecting data

Common practice when studying the kinematics related to vortex shedding is the use of imposed (or forced) oscillations [17–19] and to measure the occurring forces. With total control of the displacement one can explore a wide range of frequencies and amplitudes, contrary to the limited response behaviour observed when the mass, stiffness and the damping are fixed to certain values. Therefore, in system identification terminology, we will call the imposed motion in the y-direction (perpendicular to the incoming flow) the input to the system and the corresponding forces in the direction of oscillation, the output. To be able to generalise the results the force coefficient is used instead of the force itself:

$$c_y(t) = \frac{F_y(t)}{{}^1\!/_2 \rho U^2 D}, \tag{1}$$

with F_y the force measured in the y-direction, ρ the density of the fluid, U the unperturbed fluid velocity and D the diameter of the cylinder.

Using CFD simulations of the flow around cylinders with imposed oscillations, time series of the fluid variables are obtained. The simulations are performed using the open source CFD package OpenFOAM [20]. A transient solver called *pimpleDyMFoam* with a variable time step was used to solve the Navier-Stokes equations for an incompressible flow in a finite volume discretisation scheme [21, 22]. All simulations were performed at Re $= 100$ to ensure laminar, predominantly 2D [3], vortex formation. At this Re, a fully laminar vortex shedding takes place. Hence no turbulence model is needed. Since the vortex shedding is only 2 dimensional at Re $= 100$, a 2D mesh with the cylinder positioned $10D$ from the inlet and centred in the y-direction was used. The computational domain is $40D$ long (L) and $30D$ high (H). The top and bottom of the domain are constrained by a slip boundary condition while on the cylinder surface

itself, the velocity is set equal to the grid velocity, which follows from the cylinder motion (no-slip condition). At the inlet, a uniform velocity profile is used. The outlet is conditioned with a zero velocity gradient. The CFD models are identical to those used in [13]. Validation of the CFD models can be consulted therein.

An important aspect of nonlinear system identification is the choice of input signal. In this work we will opt for the class of input signals called random-phase multisines:

$$y(t) = \frac{1}{\sqrt{N}} \sum_{n=1}^{N} A_n \sin\left(2\pi n f_0 t + \phi_n\right) \text{ with } \phi_n \sim U[0, 2\pi[\tag{2}$$

These are periodic signals, built up out of a sum of harmonically related sine waves with a common base frequency f_0 and a set of randomly selected phases, drawn from a uniform distribution between 0 and 2π. The deliberate choice for this specific class of input signals follows from the advantage that they will also provide us with the means to quantify the amount of nonlinearity present in the data (see Section 3.1).

To focus on the influence of using the black-box or the grey-box approach, the dataset will be limited to a single amplitude level, $A_n/D = 0.30$. The dataset is in other words not optimal towards obtaining a model which is valid over a wide range of parameter space but serves as a proof of concept. The excited frequency range spans from $[{}^1\!/_{30} : {}^1\!/_{30} : 1.5] \times f_{\text{St}}$, with f_{St} being the natural vortex shedding frequency of the stationary cylinder. For imposed cylinder oscillations, the lock-in region is encountered in the neighbourhood of f_{St} [23].

2.2 Black-box PNLSS identification

The nonlinear state-space structure consists of the classical discrete time state-space equations [24] extended with nonlinear functions f and g. A linear state-space model is no more than rewriting a higher order ordinary differential equation (ODE) in a set of first order ODE's. Combined with the nonlinear functions we get:

$$\begin{cases} x(t+1) = \mathbf{A}x(t) + \mathbf{B}y(t) + f(x(t), y(t)) & \text{(3a)} \\ c_y\,(t) = \mathbf{C}x(t) + \mathbf{D}y(t) + g(x(t), y(t)). & \text{(3b)} \end{cases}$$

In the black-box approach these nonlinear functions are expressed in terms of the state variables $x(t)$ and the input which is denoted $y(t)$. The state variables are intermediate variables linking the input to the output. If a polynomial expansion is used, the nonlinear functions can be rewritten into a product of a matrix containing coefficients (**E** and **F**) and two sets of monomials (nonlinear basis functions) in $\zeta(t)$ and $\eta(t)$.

$$\begin{cases} x(t+1) = \mathbf{A}x(t) + \mathbf{B}y(t) + \mathbf{E}\zeta(t) & \text{(4a)} \\ c_y(t) = \mathbf{C}x(t) + \mathbf{D}y(t) + \mathbf{F}\eta(t), & \text{(4b)} \end{cases}$$

These nonlinear monomials are constructed by generating all possible cross products of the state variables and the input raised to a certain total degree, here denoted p. The total degree is defined as the sum of the individual exponents and this is a choice which needs to be set or experimented with. Rigorously we can write the combination of cross products as follows:

$$\zeta_{k,l_1,\ldots,l_{nx}}(t) = y^k(t) \prod_{i=1}^{n_x} x_i^{l_i}(t) \tag{5}$$

with the total degree being $k + \sum_{i=1}^{n_x} l_i \in \{0, 2, 3, ..., p\}$ with $[k, l_i] \in \mathbb{N}$ and with n_x being the number of state variables. Number-wise, if we use monomials of a total degree ranging from $p = 0$ up till $p = 5$ for a system described by $n_x = 5$ state variables, we arrive at a number of 456 basis functions (from combinatorials). The dimensions of the nonlinear coefficient matrix **E** thus grow to $n_x \times 456 = 2280$. Of these basis functions, not all will be useful in describing the data. Yet they will increase the variance on the estimate of the coefficients or even hinder finding a good estimate, in the unfortunate case.

In order to obtain estimates of all the coefficients, the following steps need to be undertaken:

- First a nonparametric estimate of the best linear approximation (BLA) is constructed. Calculation of the BLA is explained in Section 3.1.
- Using linear identification techniques, estimates of the coefficients in the linear part (**A** , **B**, **C**, **D**) are derived. The coefficients in **E** and **F** are set to zero.
- Finally, nonlinear optimisation is used to optimise all coefficients, including the nonlinear terms.

For details on the PNLSS model structure and its usage the reader is referred to [14, 25] and for applications in a variety of fields to [26–28] with the specific application for the kinematics of submerged oscillating cylinders in [13].

2.3 Grey-box PNLSS identification

Whenever prior knowledge is used to make a selection in basis functions we will consider the approach to be 'grey'. This prior knowledge can be indicative result on the type of nonlinearity, i.e. are the nonlinear function mainly odd or even, or it might include constructing a dedicated nonlinear function from the data. The first approach is based on the what is called the FAST-test and will be discussed in Section 3.2. In this Section we discuss the approach of constructing dedicated basis functions. In general, the linear state-space structure is expanded in nonlinear basis functions in terms of the output and its derivatives. These nonlinear functions can again be expanded in polynomials, leading to the following structure:

$$\begin{cases} x(t+1) = \mathbf{A}x(t) + \mathbf{B}y(t) + \mathbf{E}g(c_y(t), \dot{c}_y(t)) & \text{(6a)} \\ c_y\,(t) = \mathbf{C}x(t) + \mathbf{D}y(t) + \mathbf{F}g(c_y(t), \dot{c}_y(t)). & \text{(6b)} \end{cases}$$

In the illustrative example in Section 4.2.2 we will show that using nonlinear functions in terms of the output can lead to a more intuitive selection of the basis functions.

The identification procedure is a two step approach. First an initial estimate of the matrices of coefficients **A** , **B**, **C**, **D**, but also **E** and **F** is obtained using nonlinear subspace identification [29]. The method relies on the use of measured outputs as nonlinear regressors to construct, noniteratively a grey-box state-space model. Notice that this approach directly provides a nonlinear estimate, contrary to the black-box approach of Section 2.2.

Depending on the signal-to-noise ratio of the measured outputs, the estimates will be biased. To remove this bias nonlinear optimisation is used (second step).

3 GAINING INSIGHT INTO THE NONLINEARITY OF THE FLUID SYSTEM

From a modelling point of view, one would like to know to what extent the system at hand behaves linearly or nonlinearly. Even more insightful would be to not only have a measure

for the degree of nonlinearity, but also to be able to characterise or categorise the nonlinear behaviour in some sense. In this section these questions will be addressed by examining the variances obtained from calculation of the best linear approximation (BLA) on one hand [30], and using what is called the 'FAST'-approach [16] on the other.

The corner stone of the nonlinear analysis is the property of nonlinear systems to mix power over different frequency lines. This is in contrast to a linear system which, when it is excited by e.g. a sine wave (power at a single frequency line in the Fourier transform), will return an output only at the excited line. As an example we look at the output of a simple cubic nonlinearity when the input is a single harmonic cosine ($x(t) = \frac{e^{jwt}-e^{-jwt}}{2}$):

$$y(t) = x^3(t) \tag{7a}$$

$$= \frac{1}{8}(e^{jwt} - e^{-jwt})(e^{jwt} - e^{-jwt})(e^{jwt} - e^{-jwt}). \tag{7b}$$

From the above product we see that all possible combinations, 3 by 3, of the frequencies ω and $-\omega$ will be generated:

$$\begin{bmatrix} \omega & \omega & \omega \\ \omega & \omega & -\omega \\ \omega & -\omega & \omega \\ \omega & -\omega & -\omega \\ -\omega & \omega & \omega \\ -\omega & \omega & -\omega \\ -\omega & -\omega & \omega \\ -\omega & -\omega & -\omega \end{bmatrix} = \begin{bmatrix} 3\omega \\ 1\omega \\ 1\omega \\ -1\omega \\ 1\omega \\ -1\omega \\ -1\omega \\ -3\omega \end{bmatrix} \tag{8}$$

The spectrum of $y(t)$ is given in fig. 1. The cubic nonlinearity has generated a third harmonic

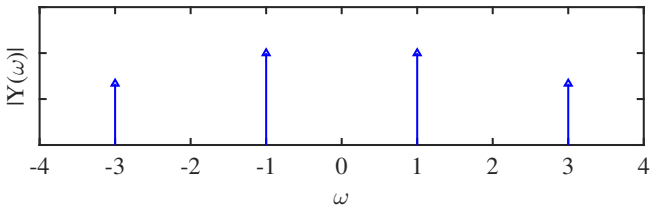

Figure 1: Frequency spectrum of the output from a cubic nonlinearity given a single harmonic input at ω.

contribution. In general we can say that odd nonlinearities will generate odd harmonic contributions while even nonlinearities will give rise to even harmonics. This property will be exploited in the FAST-approach.

3.1 Nonlinear distortions on the Best Linear Approximation

Using random phase multisines (Eq. 2) we are able to calculate an estimate of the best linear approximation (BLA) of the system. The estimate of the BLA is obtained from averaging the frequency response functions (FRF) calculated from different realisations of the random phase multisine. Since each excited frequency line is given a random phase, the contributions which are generated at other frequency lines, due to the nonlinearity, will contribute in a stochastic way. Therefore, by including multiple realisations in the averaging process, the nonlinear contributions over the different frequency lines will eventually approach a normal distribution (for

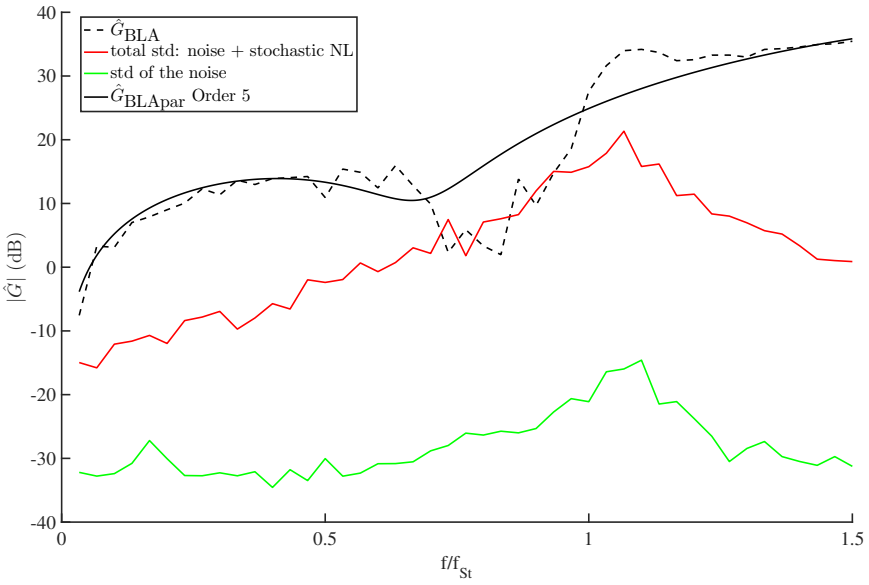

Figure 2: Nonparametric and parametric estimate of the Best Linear Approximation.

the number of excited lines going to infinity but in practice as many as 20 lines works already quite well [16]). Averaging yields a zero expected value for the nonlinear distortions and what will remain can be called the best linear approximation. The variance associated with this mean FRF will be a measure for the nonlinear distortions present at a given frequency line. If the measurements are noisy, we obtain the total variance which is the sum of the nonlinear distortions and the noise.

In Fig. 2 nonparametric and a parametric estimate, obtained from a model scan using the FDIDENT[1] toolbox in MATLAB, of the BLA are plotted. A finite impulse response model of 5^{th} order was selected. Details can be found in [13]. A considerable level of total distortions, reaching as high as the function itself in the region around f_{St}, indicates a high level of nonlinear distortions.

3.2 The 'FAST'-approach

The objective of the FAST-approach is to characterise the type of nonlinearity, i.e. whether even or odd nonlinearities are present. The approach relies on the usage of a specifically constructed signal called random odd multisines. A random odd multisine is again a sum of harmonically related sines with randomly selected phases but compared to the previously used (full) random phase multisines, 2 constraints are added on the excited frequency lines. For random odd, only the odd frequency lines are excited, excluding one line for every bin of 4 odd lines. The odd lines which are excluded are called detection lines and the position of these lines within a bin of 4 odd lines is chosen randomly.

From the previous sections we know that when analysing the output of a system, the linear contributions will only be present at the excited lines. At the even lines, there can be contributions following from even nonlinearities only, since no even lines are excited in a random odd multisine. Similarly, at the odd unexcited lines (detection lines), there can only be contributions from

[1] http://vubirelec.be/knowledge/downloads

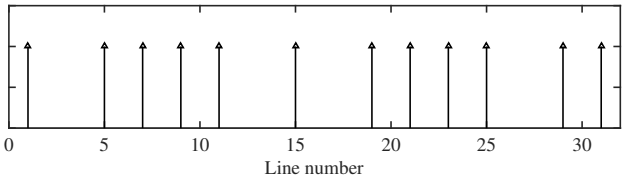

Figure 3: Example of the DFT spectrum of a random odd multisine.

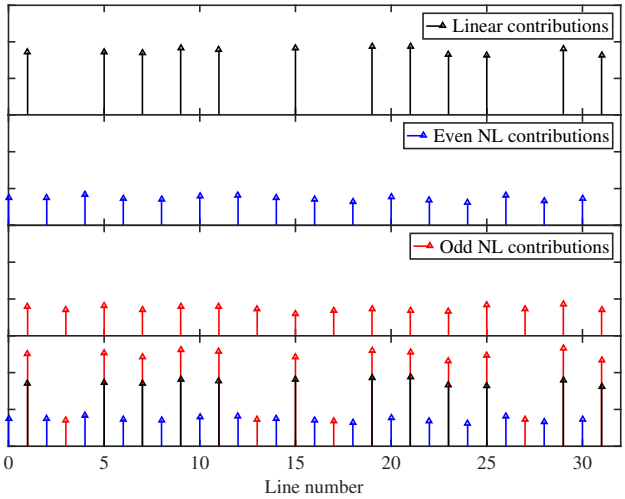

Figure 4: The different output contributions that can follow from exciting a nonlinear system with a random odd multisine.

odd nonlinearities. But also at the excited odd lines there can be odd nonlinear contributions, hence the odd excited lines will contain the sum of the linear and the odd nonlinear contributions. In Fig. 3 the DFT of a random odd input signal is shown. Fig. 4 shows the different contributions found in the output, first separately, and then summed together in the case the random odd input signal would have passed through a nonlinear system containing both odd and even nonlinearities.

The same approach is applied to characterise the nonlinear distortions of c_y. Fig. 5 shows the DFT output spectra at the amplitude level $A/D = 0.30$, for an imposed cylinder motion of a random odd multisine. We observe that only odd nonlinear contributions are present in the output signal. The even contributions are as low as the noise floor. These observations will guide us during the selection of nonlinear basis functions in Section 4.1.

4 ESTIMATION RESULTS

In this Section we compare how well we are able to tune a PNLSS model to a selection of training data, given their selection of basis functions. As was discussed in 2.1 we use random-phase multisine data to train the model. A number of six realisations were applied and transients were dealt with by including an extra period at the beginning of each realisation and disregarding it later when optimising the coefficients.

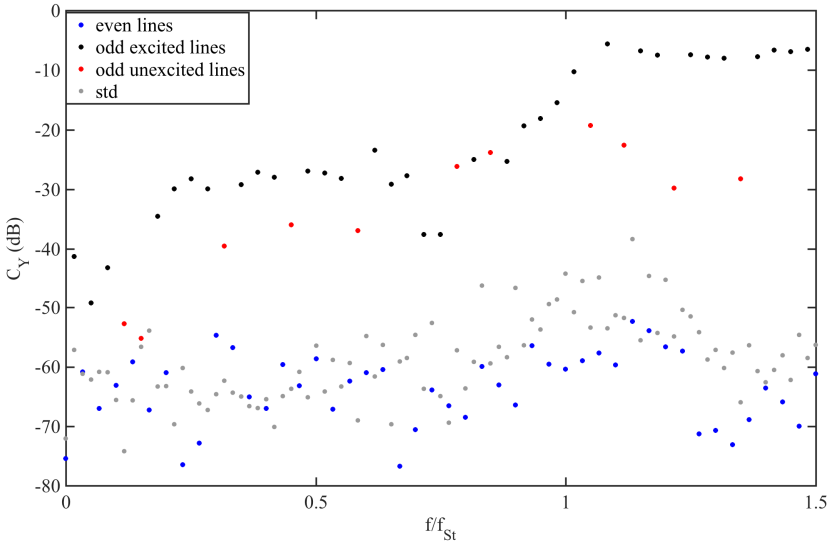

Figure 5: Characterising the type of nonlinearity using the FAST-approach.

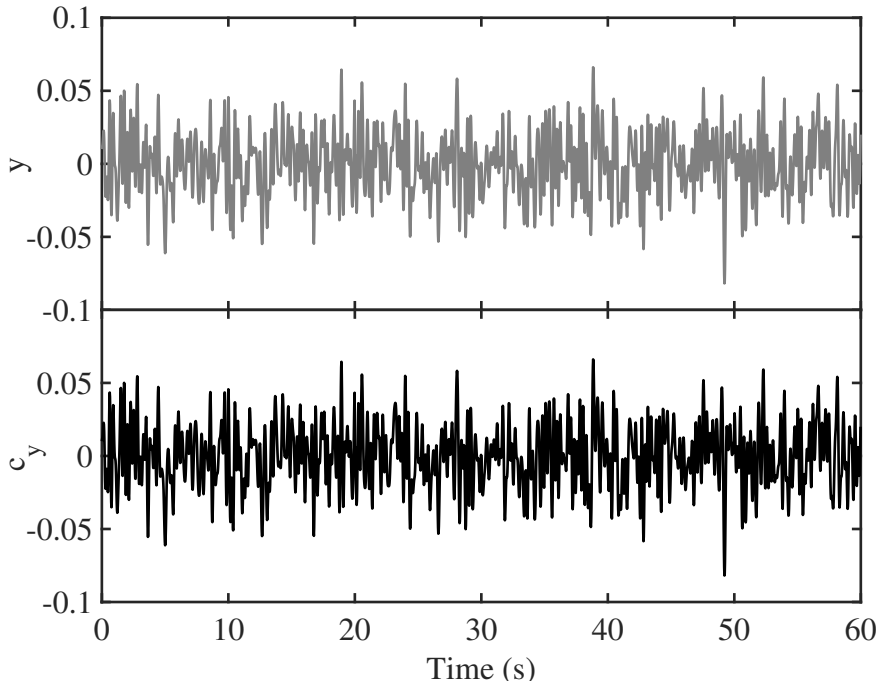

Figure 6: Input and output of the training dataset. The set includes 6 realisations of a random phase multisine exciting the frequency band $[{}^{1}/_{30} : {}^{1}/_{30} : 1.5] \times f_{\mathrm{St}}$ at $A/D = 0.30$

4.1 Black-box modelling

In the black-box modelling approach we include all monomials from nonlinear degree 0 up to 5 in η and ζ of Eq. (6). We start from the BLA and run the nonlinear optimisation routine. Errors are expressed in terms of their relative rms values:

$$e_{\text{rms}} = \sqrt{\frac{1}{N}\frac{\sum_{t=0}^{N}(c_y(t) - c_{y\text{mod}}(t))^2}{\sum_{t=0}^{N} c_y(t)^2}}, \tag{9}$$

where c_y corresponds to the true output and $c_{y\text{mod}}$ is the modelled output. The results of the linear and the final nonlinear model are listed in table 1.

Model	e_{rms}
BLA	0.43
PNLSS black-box	0.078

Table 1: Estimation results from the black-box modelling approach.

Clearly a considerable improvement can be achieved by estimating a nonlinear model. This could be expected from the high level nonlinear distortions found from calculation of the BLA.

4.2 Grey-box modelling

In Section 4.2.1 we repeat the procedure of Section 4.1 but now including the results from the FAST-approach. In Section 4.2.2 the procedure of the output nonlinear basis functions is illustrated on an example system related to the fluid system previously considered.

4.2.1 Including prior knowledge from FAST

From the FAST-test we learned that the fluid forces were governed by odd nonlinear effects therefore, during this approach we only consider the nonlinear degrees 0,3,5. The BLA is identical to the black-box case.

Model	e_{rms}
BLA	0.43
PNLSS black-box	0.109

Table 2: Estimation results from the grey-box modelling approach.

Compared to the black-box approach the model estimate performs slightly worse. Since the search space has been reduced it has become harder to accurately tune to the data, i.e. arrive in a low local minimum of the cost function. We will however see in Section 5.2.1 that the opposite will be true when assessing the quality of the model on validation data.

4.2.2 Illustration of output nonlinearties

The illustration of the output nonlinear basis functions approach is done on a system which resembles to a large extent the fluid system previously studied. The system is described by the

Van der Pol equation: [31]:

$$\ddot{c}_y + \mu\Omega_{\text{aut}}(c_y^2 - 1)\dot{c}_y + \Omega_{\text{aut}}^2 c_y \ = \dot{y}. \tag{10}$$

This system also produces autonomous oscillations and has a synchronisation region depending on excitation frequency and amplitude, just as in the case of the fluid system. In Eq. (10), Ω_{aut} denotes the autonomous angular oscillation frequency, c_y again represents the output and in this case the derivative of the displacement, $\dot{y}$ is used as the input and the Van der Pol coefficient μ is set to 0.3 [32].

From Eq. (10) we are able to generate random phase multisine data from time integration with the built in solver ODE45 in MATLAB. Using this data we are able to repeat the fully black-box approach and easily illustrate the output nonlinear approach. The reason for illustrating the output nonlinear approach on data of a known equation is that now it can be clearly seen that the nonlinear contributions stem from a polynomial in terms of the output and its derivative, in this case c_y^2 and $\dot{c}_y$. The estimation result on 7 realisation of a random phase multisine at an amplitude level $A = 15$ for the right hand side of Eq. (10) reaches as low as the noise floor for both the black-box as the output nonlinear grey-box approach.

Even though no noise was added, the data still suffer from disturbances originating to time integration errors. These will pop-up in the noise floor.

5 VALIDATION RESULTS

In this Section both models estimated on data of the fluid system and the models estimated on data of the Van der Pol equation are validated by simulating the output to a new unseen random phase multisine realisation.

5.1 Black-box modelling

The validation set used is composed out of an unseen random-phase multisine of the same frequency content as during training but a lower amplitude level of $A/D = 0.285$. The error of the estimated black-box PNLSS model is plotted together with the error of the linear estimate and the noise floor (Fig. 7).

The error which is obtained corresponds to $e_{\text{rms}} = 0.29$.

5.2 Grey-box modelling

5.2.1 Including prior knowledge from FAST

For the grey-box validation the same validation signal is applied. This model was constructed using the prior knowledge from the FAST-test, hence only the nonlinear degrees 0, 3 and 5 were used. The results are shown in Fig. 8.

The error which is obtained corresponds to $e_{\text{rms}} = 0.12$. The true output along with the error is once more plotted in the time domain in Fig. 9.

It can be noticed that even though the black-box approach performed better in terms of estimation error, it is clearly off on the validation part. Reasonably good results are obtained when

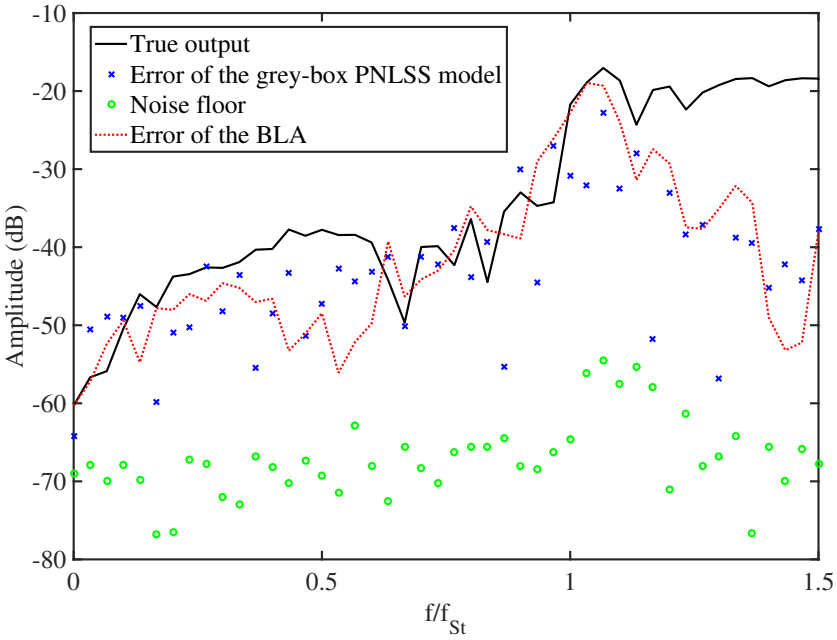

Figure 7: Validation of the black-box model to an unseen random-phase multisine of c_y from CFD.

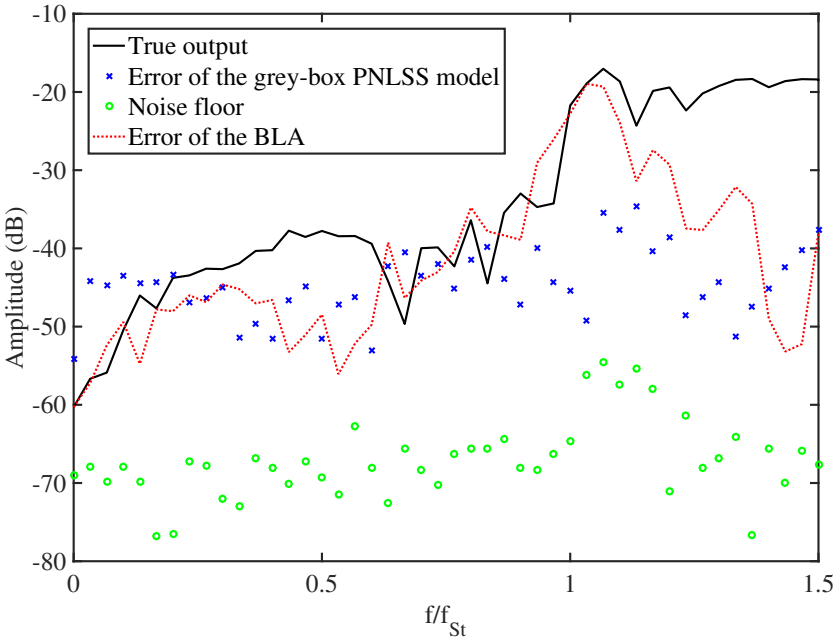

Figure 8: Validation of the grey-box model, only including the nonlinear degrees 0, 3 and 5, to an unseen random-phase multisine of c_y from CFD.

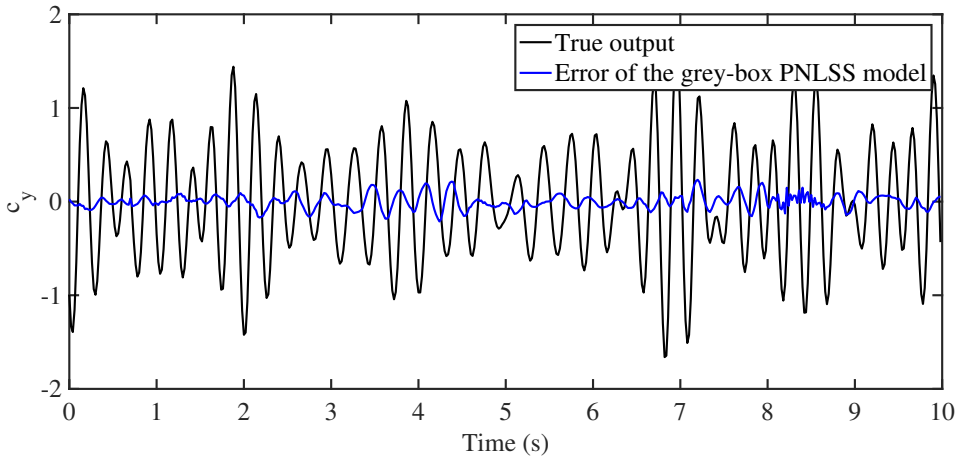

Figure 9: Validation of the grey-box model, only including the nonlinear degrees 0, 3 and 5, to an unseen random-phase multisine of c_y from CFD in the time domain.

the correct type of basis functions is selected, $e_{\text{rms}} = 0.12$, especially taking into account the $e_{\text{rms}} = 0.109$ on the estimation data. Choosing the correct type of nonlinear degrees can thus lower the possibility of overfitting on the training data.

5.2.2 Illustration of output nonlinearties

On the less complex data, generated from the Van der Pol equation we compare the black-box approach to the output nonlinear basis functions approach (Fig. 10 and Fig. 11). We notice that in this case both approaches reach almost to the noise floor with a slightly better result for the output nonlinearities. This real benefit, however, is made in terms of the amount of coefficients needed. Since the exact basis functions can be constructed using the output only one is needed whereas the black-box approach contains all the combinatorial options of products between the state variables and the input of total degree 3.

6 CONCLUSION

We have shown that for the purpose of modelling fluid forces using a PNLSS model structure, it is helpful first to characterise the type of nonlinearity using the FAST-test. Doing so, a deliberate choice of basis functions can be selected. With respect to a black-box approach of equal degree, this choice will restrict the search space, possibly leading to an increased error on the estimation data. On the other hand, an improvement on the validation data was observed when the correct degrees were selected. Moreover we haven shown that using dedicated basis functions, constructed in terms of the output, one can considerably reduce the amount of coefficients in the model. These results have been found for a system closely related to the fluid force system, namely the Van der Pol equation. Since the Van der Pol equation has been frequently used to model fluid force behaviour of VIV nature, the nonlinear term present therein can serve as starting point in the search for a dedicated nonlinear basis function to model the fluid forces occurring for oscillating cylinders in a fluid flow.

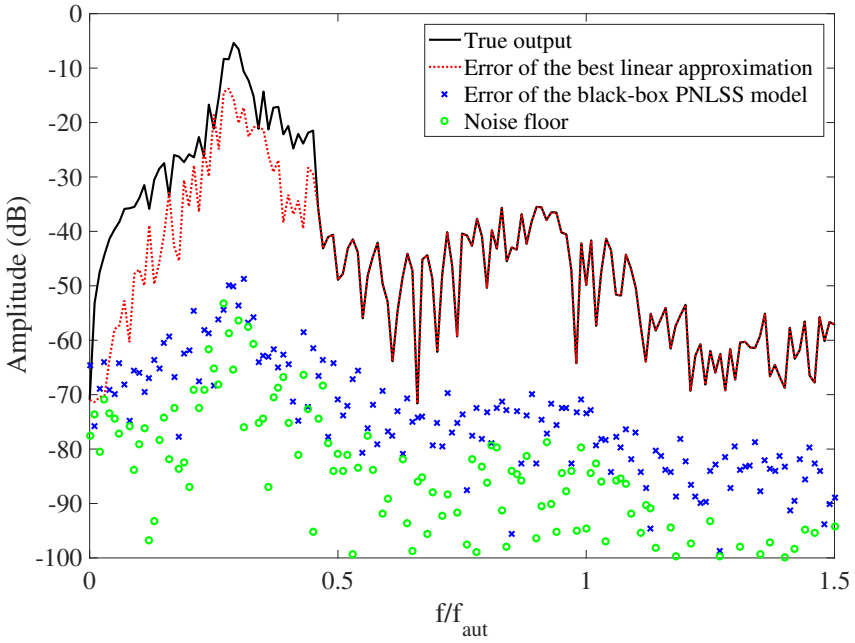

Figure 10: Validation of the black-box model estimation on the Van der Pol data.

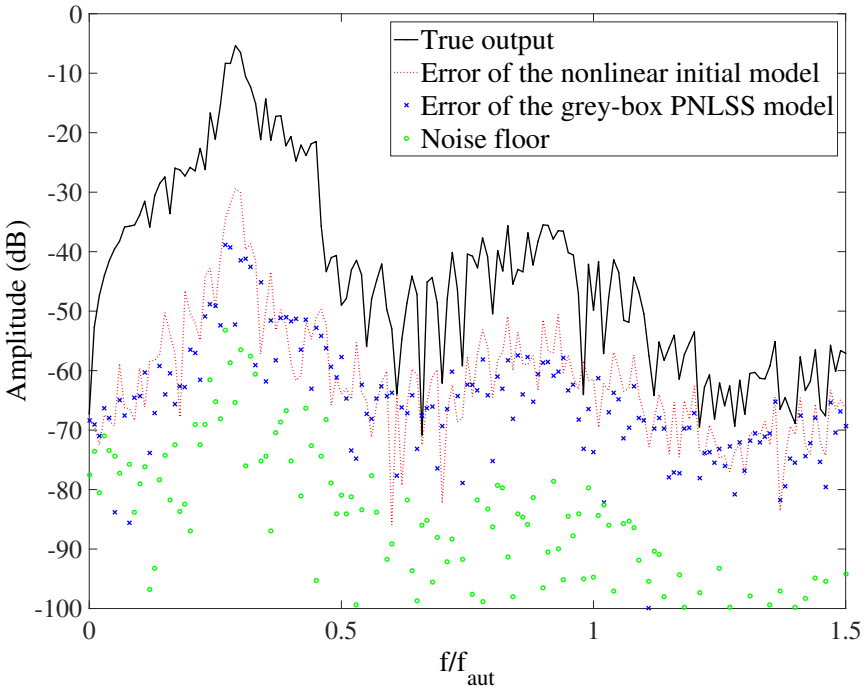

Figure 11: Validation of the grey-box model, estimated using basis functions in terms of the output, on data of the Van der Pol equation.

ACKNOWLEDGEMENTS

This work was supported in part by the Fund for Scientific Research (FWO-Vlaanderen), by the Flemish Government (Methusalem), the Belgian Government through the Inter-university Poles of Attraction (IAP VII) Program, and by the ERC advanced grant SNLSID, under contract 320378.

7 REFERENCES

[1] Zdravkovich, M. M. (1991). *Flow around circular cylinders, Volume 1: Fundamentals*, vol. 1. Oxford University Press.

[2] Sen, S., Mittal, S., and Biswas, G. (2009). Steady separated flow past a circular cylinder at low reynolds numbers. *Journal of Fluid Mechanics*, 620, 89–119.

[3] Williamson, C. H. K. (1996). Vortex dynamics in the cylinder wake. *Annual Review of Fluid Mechanics*, 28, 477–539.

[4] Sarpkaya, T. (2004). A critical review of the intrinsic nature of vortex-induced vibrations. *Journal of Fluids And Structures*, 19, 389–447.

[5] Williamson, C. and Govardhan, R. (2004). Vortex-induced vibrations. *Annual Review of Fluid Mechanics*, 36, 413–455.

[6] Khalak, A. and Williamson, C. H. K. (1999). Motions, forces and mode transitions in vortex-induced vibrations at low mass-damping. *Journal Of Fluids And Structures*, 13, 813–851.

[7] Bearman, P. (1984). Vortex shedding from oscillating bluff bodies. *Annual Review of Fluid Mechanics*, 16, 195–222.

[8] Gabbai, R. D. and Benaroya, H. (2004). An overview of modeling and experiments of vortex-induced vibrations of circular cylinders. *Journal of Sound and Vibration*, 282, 575–616.

[9] Bishop, R. E. D. and Hassan, A. Y. (1963). The lift and drag forces on a circular cylinder oscillating in a flowing fluid. In *Proceedings of the Royal Society of London A*, vol. 227. pp. 51–75.

[10] Blackburn, H. M. and Henderson, R. D. (1999). A study of two-dimensional flow past an oscillating cylinder. *Journal of Fluid Mechanics*, 385, 255–286.

[11] Cicolani, L., da Silva, J., Duque, E., et al. (2004). Unsteady aerodynamic model of a cargo container for slung-load simulation. *Aeronautical Journal*, 108(1085), 357–368.

[12] Runacres, M., De Troyer, T., Shirzadeh, R., et al. (2013). System identification of the kinematics of an oscillating cylinder using wake velocities. *Journal of Fluids and Structures*, 41, 57–63.

[13] Decuyper, J., De Troyer, T., Runacres, M., et al. (2017). Nonlinear state-space modelling of the kinematics of an oscillating circular cylinder in a fluid flow. *Mechanical Systems and Signal Processing*, 98, 209–230.

[14] Paduart, J., Lauwers, L., Swevers, J., et al. (2010). Identification of nonlinear systems using polynomial nonlinear state space models. *Automatica*, 46, 647–657.

[15] Noël, J. P., Esfahani, A. F., Kerschen, G., et al. (2017). A nonlinear state-space approach to hysteresis identification. *Mechanical Systems and Signal Processing*, 84, 171–184.

[16] Pintelon, R. and Schoukens, J. (2001). *System Identification: A Frequency Domain Approach.* IEEE Press.

[17] Govardhan, R. and Williamson, C. H. K. (2000). Modes of vortex formation and frequency response of a freely vibrating cylinder. *Journal of Fluid Mechanics*, 420, 85–130.

[18] Morse, T. and Williamson, C. (2009). Prediction of vortex-induced vibration response by employing controlled motion. *Journal of Fluid Mechanics*, 634, 5–39.

[19] Carberry, J., Sheridan, J., and Rockwell, D. (2005). Controlled oscillations of a cylinder: forces and wake modes. *Journal of Fluid Mechanics*, 538, 31–69.

[20] Greenshields, C. J. (2016). *OpenFOAM User Guide*. OpenFOAM Foundation Ltd., 4 ed.

[21] Islam, T., Rakibul Hassan, S., Ali, M., et al. (2014). Finite volume study of flow separation phenomena for steady flow over a circular cylinder at low reynolds number. *Procedia Engineering*, 90, 282–287.

[22] Versteeg, H. and Malalasekera, W. (2007). *An introduction to computational fluid dynamics: the finite volume method*. Prentice Hall.

[23] Kumar, S., Navrose, and Mittal, S. (2016). Lock-in in forced vibration of a circular cylinder. *Physics of Fluids*, 28, 113605.

[24] Kailath, T. (1980). *Linear Systems*. Englewood Cliffs, New Jersey: Prentice-Hall.

[25] Paduart, J. (2008). *Identification of nonlinear systems using Polynomial Nonlinear State Space models*. Ph.D. thesis, Vrije Universiteit Brussel.

[26] Relan, R., Firouz, Y., J., T., et al. (2016). Data driven nonlinear identification of li-ion battery based on a frequency domain nonparametric analysis. *IEEE Transactions on control systems technology*, PP(99), 1–8.

[27] Widanage, W. D., Stoev, J., Van Mulders, A., et al. (2011). Nonlinear system-identification of the filling phase of a wet-clutch system. *Control Engineering Practice*, 19, 1506–1516.

[28] Coen, T., Paduart, J., Anthonis, J., et al. (2006). Nonlinear system identification on a combine harvester. In *Proceedings of the American control conference*. Minneapolis, Minnesota, USA, pp. 3074–3079.

[29] Noël, J. P. and Kerschen, G. (2013). Frequency-domain subspace identification for nonlinear mechanical systems. *Mechanical Systems And Signal Processing*, 40, 701–717.

[30] D'Haene, T., Pintelon, R., Schoukens, J., et al. (2005). Variance analysis of frequency response function measurements using periodic excitations. *Transactions on Instrumentation and Measurement*, 54(4), 1452–1456.

[31] Van der Pol, B. (1926). Relaxatie-trillingen. *Tijdschrift van het Nederlandsch radiogenootschap*, 3, 25–40.

[32] Facchinetti, M. L., de Langre, E., and Biolley, F. (2004). Coupling of structure and wake oscillators in vortex-induced vibrations. *Journal of Fluids And Structures*, 19, 123–140.

8 COPYRIGHT STATEMENT